Direct numerical simulation of hot jets

By M. C. Jacob[1]

1. Motivation and objectives

1.1 Background

The ultimate motivation of this work is to investigate the stability of two dimensional heated jets and its implications on aerodynamic sound generation from data obtained with direct numerical simulations (DNS). As pointed out in our last report, these flows undergo two types of instabilities, convective or absolute, depending on their temperature. We also described the limits of earlier experimental and theoretical studies (*e.g* Yu & Monkewitz (1989) and Huerre & Monkewitz (1990)) and explained why a numerical investigation could give us new insight into the physics of these instabilities. The aeroacoustical interest of these flows was also underlined.

In order to reach this goal, we first need to succeed in the DNS of heated jets. Our past efforts have been focused on this issue which encountered several difficulties. Our numerical difficulties are directly related to the physical problem we want to investigate since these absolutely or almost absolutely unstable flows are by definition very sensitive to the smallest disturbances and are very likely to reach non-linear saturation through a numerical feed-back mechanism. As a result, it is very difficult to compute a steady laminar solution using a spatial DNS. A steady state was reached only for strongly co-flowed jets (Jacob (1991)), but these flows are almost equivalent to two independent mixing layers. Thus they are far from absolute instability and have much lower growth rates.

1.2 Preliminary simulations

Nevertheless, DNS of convectively and absolutely unstable jets show some interesting features which qualitatively indicate that these two types of flows respond differently to the transient waves generated at the beginning of the simulations. Two cases were initially computed with the Poinsot-Lele code (Lele (1992), Poinsot & Lele (1992)): for both cases, the inflow jet-diameter $D = 10\delta_\omega$, where δ_ω is the vorticity thickness, the inlet U-velocity uses a top-hat profile given by Yu & Monkewitz (1989) to which a co-flow $U_2 = 0.05U_1$ has been added, the inlet V-velocity is zero, and the inlet temperature profile is given by the Crocco-Buseman relation (Sandham & Reynolds (1989)). For numerical reasons, the computation is carried out at a low Reynolds number ($Re_D = 2000$), which is still high enough to avoid significant viscous effects. The dimensions of the computational domain are: $L_x = 60\delta_\omega$ and $L_y = 40\delta_\omega$. Time is scaled by δ_ω/c, c being the speed of sound outside the flow. The centerline Mach number has been set to $M_1 = 0.4$ in order to

1 Currently at Ecole Centrale de Lyon, France

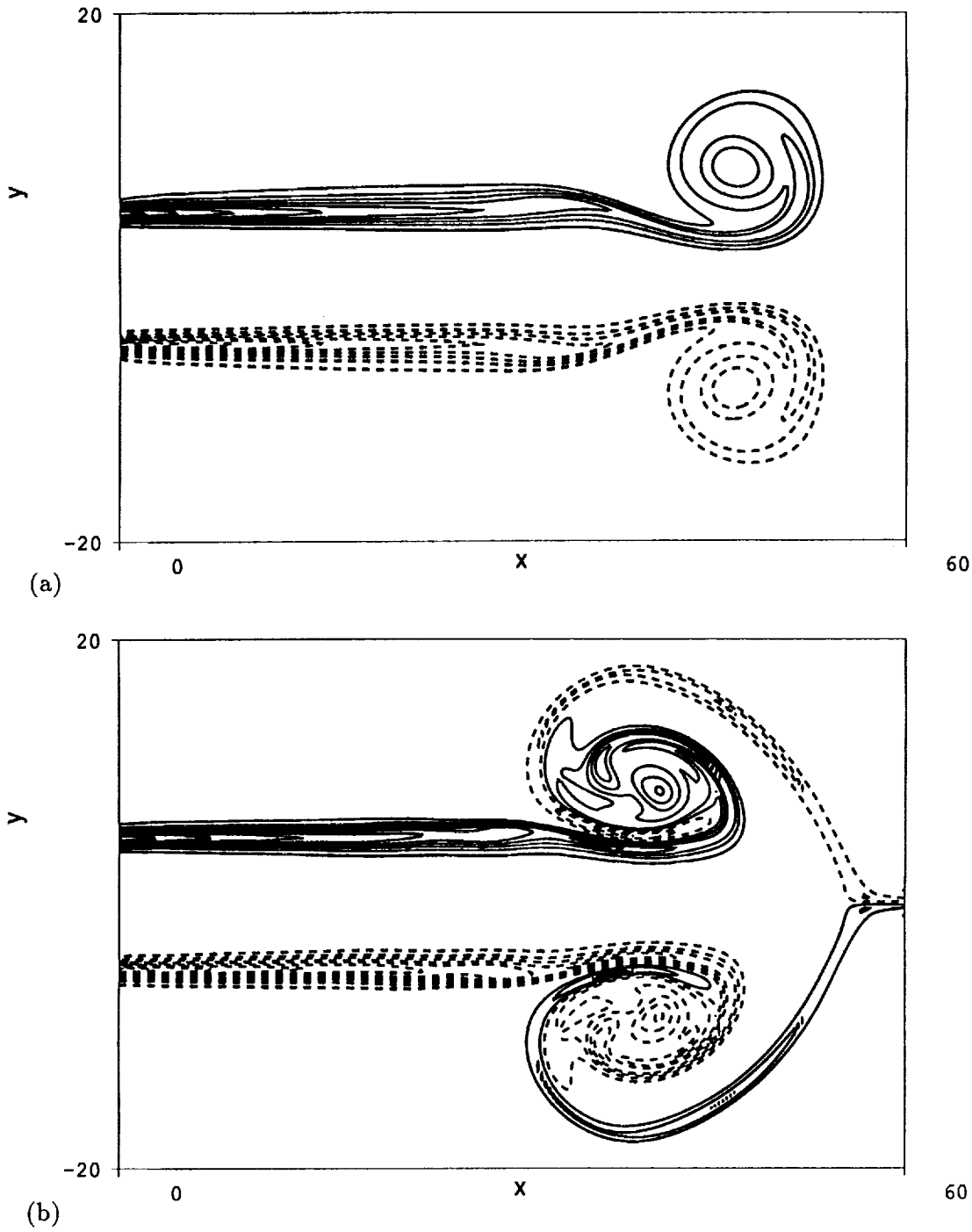

FIGURE 1. Vorticity contours. (a): Convectively unstable jet ($S = 1.0$) at time= 288 with 10 contours levels : min= -0.3799 , max= 0.3799; (b): Absolutely unstable jet ($S = 0.5$) at time= 314 with 10 contour levels : min= -0.3772 max= 0.3772. Dashed lines are used for negative values in both plots.

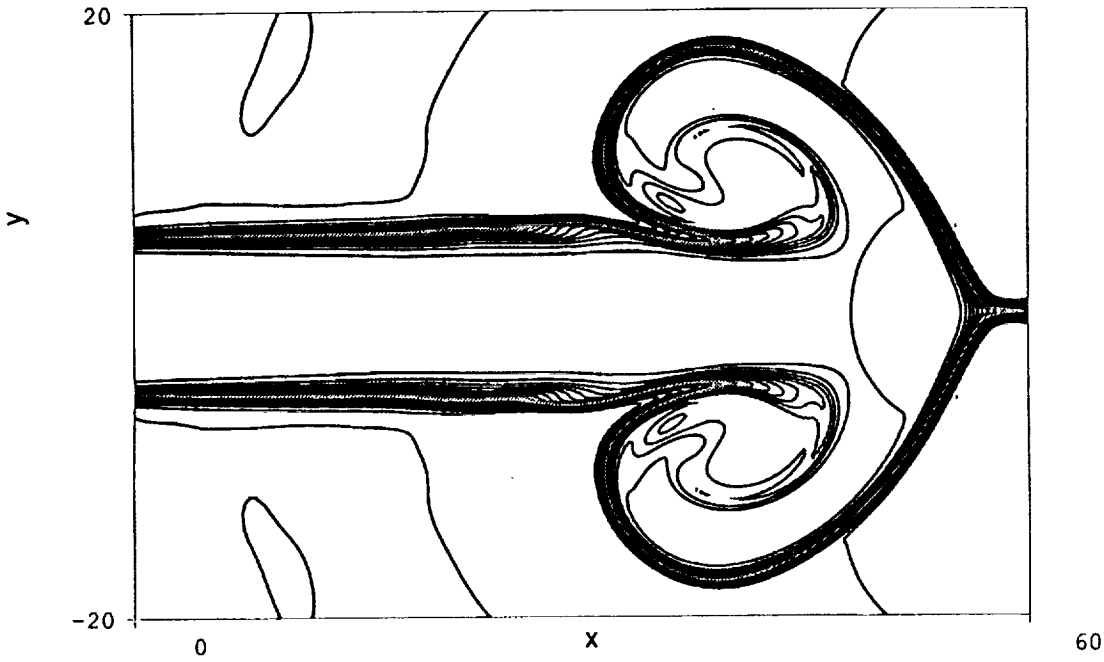

FIGURE 2. Density contours of the absolutely unstable jet ($S = 0.5$) at Time= 314 with 10 contour levels : min= 0.9697 , max= 2.0624 :the two shear layers are interacting.

limit compressibility effects. The two cases differ only by their temperature profiles: one is a cold (convectively unstable) jet, and the other is a heated absolutely unstable jet which has a temperature ratio $S = 0.5$ between the external temperature (T_2) and the centerline temperature (T_1). In both cases, the transient generates a pair of vortices on each shear layer. Figure 1 shows a typical vorticity field for each case. The snapshots are taken just after the first vortex leaves the domain and shortly before the largest structure of the transient reaches the outflow. It is clear that the vortices of the two mixing layers interact for the absolutely unstable case, whereas they seem to evolve independently in the cold jet. The corresponding density contour plot of the hot jet shows how the two shear layers interact in the transient perturbation (see Figure 2).

A theoretical explanation of this may be given in terms of vorticity dynamics: in the cold jet, pressure and density gradients are primarily created by the vortices. They are both predominately radial and, therefore, parallel. Thus the baroclinic term of the vorticity equation is negligible for a cold jet, and the evolution of the instability depends mainly on the velocity shear. In the hot jet, however, the baroclinic term is no longer negligible because the temperature stratification results in a cross-stream density gradient which combines with streamwise components of the pressure gradient and redistributes vorticity. According to this interpretation, vorticity should be decreased on the downstream side of a vortex and increased on the upstream side. This would explain qualitatively the difference between the vortical structures of Figures 1(a) and 1(b) which correspond to the upstream end of

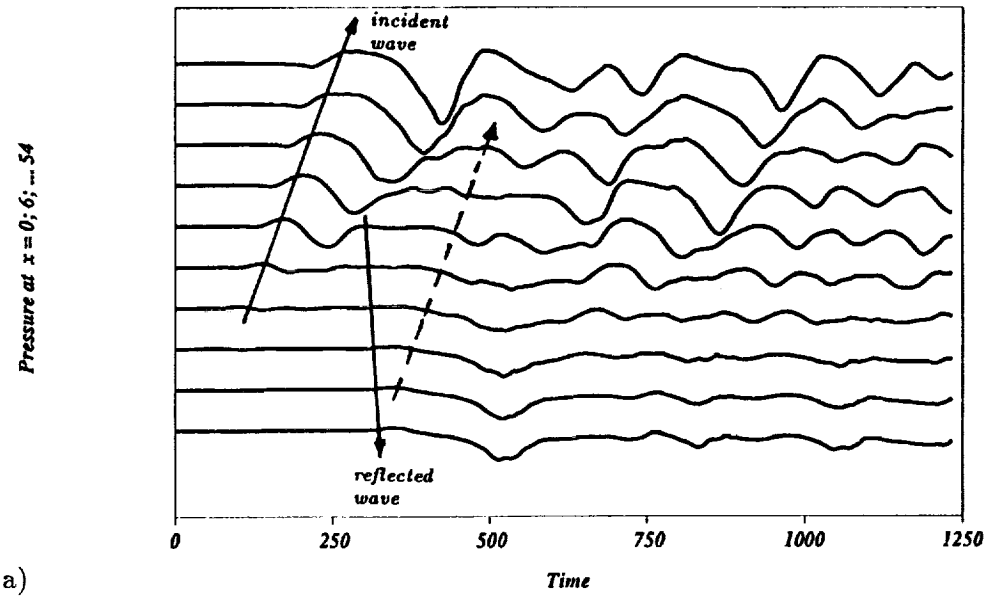

(a)

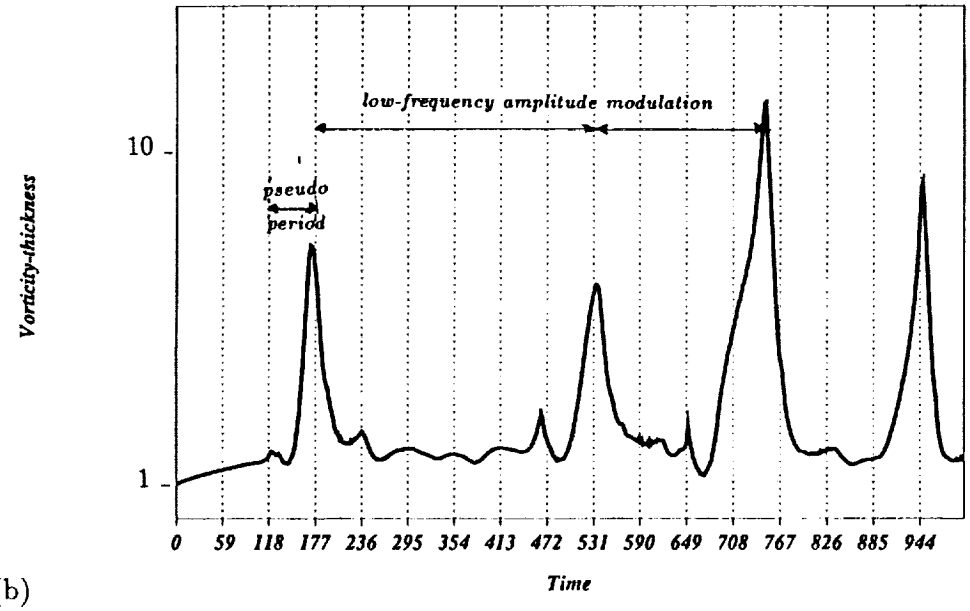

(b)

FIGURE 3. Flow history of the absolutely unstable jet ($S = 0.5$). (a): Pressure outside the jet at different x-locations; (b):Vorticity thickness history at x= 30.

the initial (vortical) disturbances for each case. Near the outflow the corresponding boundary conditions generate a strong pressure perturbation (see Figure 3(a)) which further modifies the baroclinic term.

In both cases, the disturbances are so strong that they reflect strong waves at the outflow which generate new, stronger perturbations at the inflow. Hints to this numerical feedback mechanism can be seen for the hot jet in Figure 3(a), although the upstream traveling waves are interfering with the continuously generated downstream traveling waves. This mechanism appears more strikingly in more stable flows in which fewer waves are propagating simultaneously (mixing layers, strongly co-flowed jets *etc.*).

We choose not to report this case since this feedback is already well documented elsewhere(*e.g.* Poinsot & Lele (1992)). The amplitude of the disturbances eventually saturates, and the flow reaches a pseudo-periodic state as shown in Figure 3(b). Furthermore, by comparing the two jets, we found that the pseudo-period (≈ 60 normalized time units) is roughly the same for both flows. It is also invariant to doubling the domain length which means that it is not due to a resonance of the computational domain. The low-frequency amplitude modulation is related to the biggest structures (as the one shown in Figure 1).

1.3 Objectives of the current research

Several questions arise from these results:

- What other physical conclusions can be drawn from these preliminary calculations?
- Does the observed pseudo-frequency correspond to a jet mode which is excited by ambient (numerical) noise or to a purely numerical artifact?
- Is there any possibility of controlling this frequency?
- Is there any hope of controlling the transient and thus the resulting feedback?
- Could the transient be reduced in order to reach a steady state, or are the self-sustained instabilities inherent to the jet dynamics?

In order to answer these questions, we have carried out various tests concerning both the numerics (boundary conditions, initial conditions) and the physics (stability analysis, forcing at eigen-frequencies, co-flow). In the following section, we shall give a summary of this investigation which was performed between November 1991 and June 1992.

2. Accomplishments and current work

2.1 Co-flowed jets

As previously mentioned, a steady laminar solution has been found for jets with a significant co-flow (see Figure 4). Figure 4(b) shows slight disturbances at the inlet which are due to an unrealistic V-velocity estimate ($V = 0$) at the inflow. In §2.4.1, we will see how this can be improved. For such a strongly co-flowed jet, several codes available at CTR (the Poinsot-Lele code with one dimensional boundary conditions and the Colonius code with obliquely non-reflecting first order

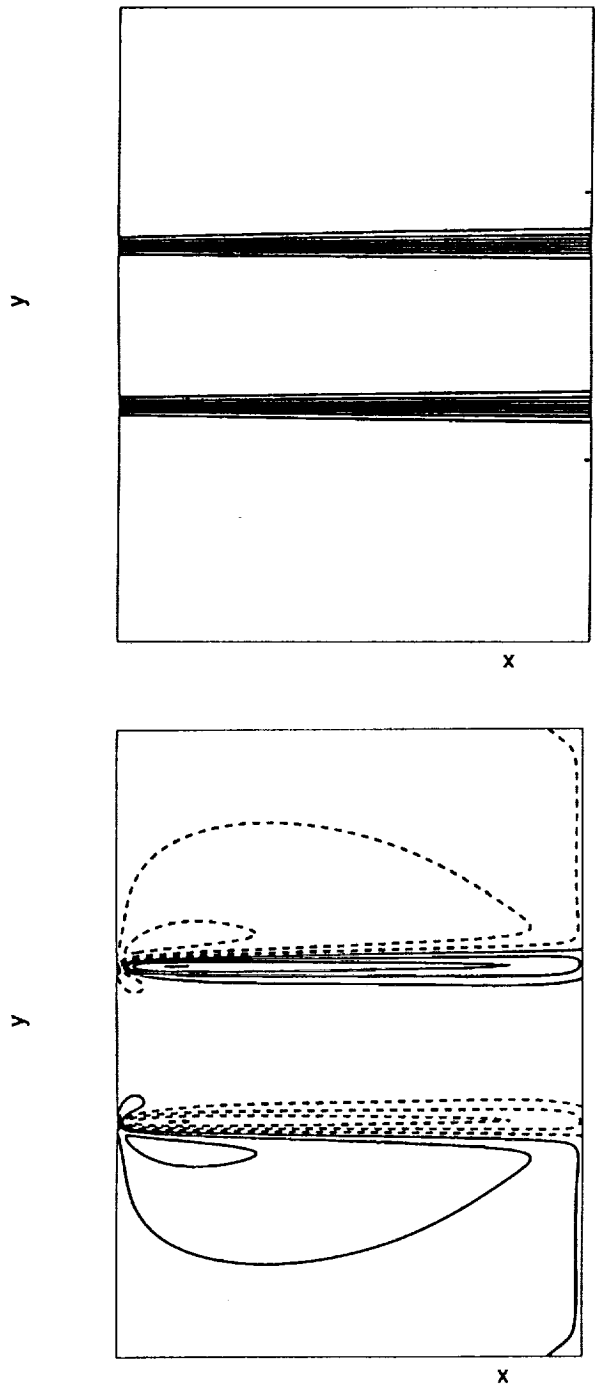

FIGURE 4. Co-flowed cold jet ($U_2 = 0.5U_1$; $L_x = 30$). Contour plots of: (a): U-velocity at time= 308 10 contour levels : min= 0.18 , max= 0.4; (b): V-velocity at time= 308. 10 contour levels : min= −0.001019 , max= 0.001019; Dashed lines are used for negative values in (b) only.

Giles boundary conditions (Colonius *et al.* (1991), Giles (1990)) converge with a comparable accuracy to the steady-state. This is not surprising since the co-flow reduces the relative shear with respect to the convection velocity and thus stabilizes the jet. Therefore, the transient is less amplified by the flow and possibly less intense initially. We found that the minimal co-flow required to reach a steady laminar state is at least $U_2 = 0.25U_1$ for cold jets and increases significantly along with the jet temperature. It is therefore legitimate to examine if absolute instabilities might still be observed given such constraints.

2.2 Linear Inviscid Incompressible Stability Analysis(LIISA)

In order to determine the specific impact of co-flows on the instability, a LIISA was carried out for 2D heated co-flowed jets. The restriction to inviscid incompressible flows is justified by the fact that the mechanism of the Kelvin-Helmholtz instability is inviscid and that compressibility effects are not significant for low Mach numbers. (We have verified that the results of our DNS code remain of the same type at lower Mach numbers and for inviscid flows.)

2.2.1 Absolute instability limit

The (complex) absolute frequency ω_0 (this is a freqency for which there exists a complex wavenumber k_0 such that : $[\partial\omega_0/\partial k](k_0) = 0$) has been determined by solving the complex dispersion relation $D(k_0, \omega_0) = 0$ of the linear stability problem. The dispersion relation is solved numerically *via* the Rayleigh equation for stratified flows using a finite difference scheme along with a minimization technique (Trouvé (1988)). The strategy for determining the zero group-velocity solution is described by Monkewitz & Sohn (1986). The values of ω_0 for various co-flows (U_2) and temperature ratios ($S = T_2/T_1$) are plotted in the (ω_r, ω_i) plane in Figure 5.

According to the linear stability theory, the absolutely unstable flows correspond to the cases where the imaginary part ω_i^0 of ω_0 is positive. It is also interesting to point out the shape of the spatial amplification in the vicinity of the absolute frequency for the case S = 0.5 (see Figure 6). According to Bers (1983), this might be due to an interchange between the two branches of the dispersion relation.

The important conclusion from this study is that absolute instability occurs only if the co-flow remains less than 1/10 of the centerline velocity. Thus the cases for which a steady laminar solution can be obtained *via* DNS correspond precisely to flows which are not likely to become absolutely unstable even by strong heating. Hence we must look for another way to reach a steady state or at least to control the transient generated when the DNS is started.

2.2.2 Forcing

One possible way to control the transient in the DNS of convectively unstable jets is to force the flow at its most unstable frequency; indeed, if the forcing level is comparable to the ambient noise, the flow will lock on the forcing frequency. This can, of course, only be achieved if the transient is not so intense that the non-linear saturation of the jet is reached. The LIISA is used to determine the spatial amplification curves: $-\alpha_i = f(\omega_r)$ for different co-flows (see Figure 6) and

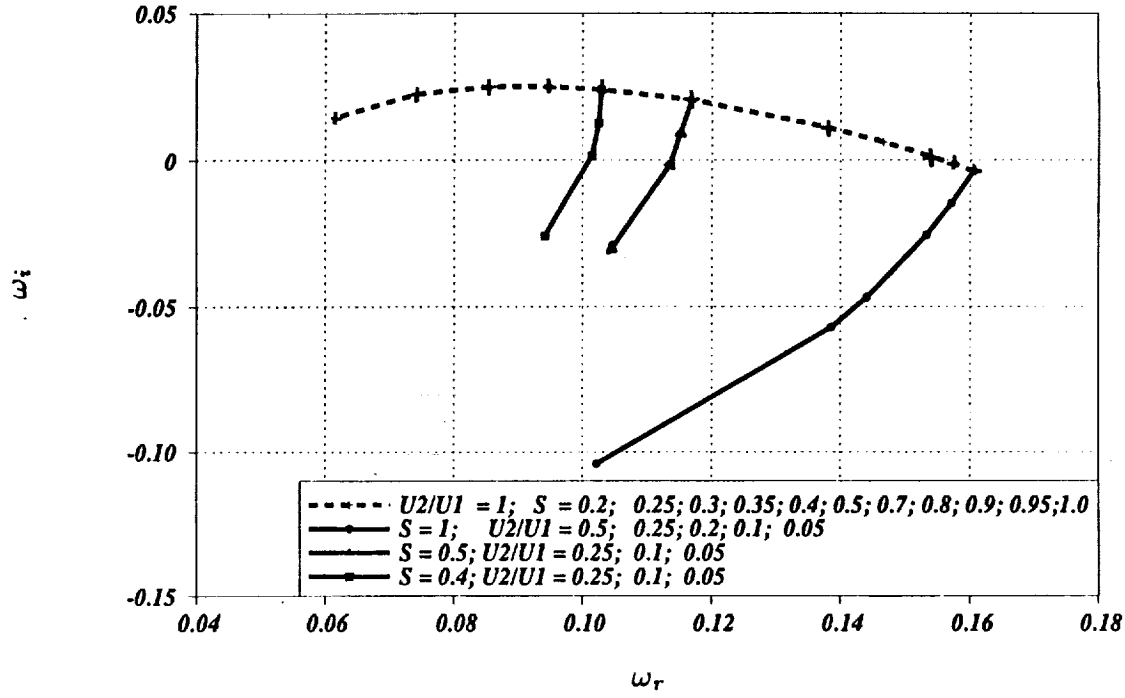

FIGURE 5. Absolute frequency for various co-flows (U_2) and temperature ratios(S).

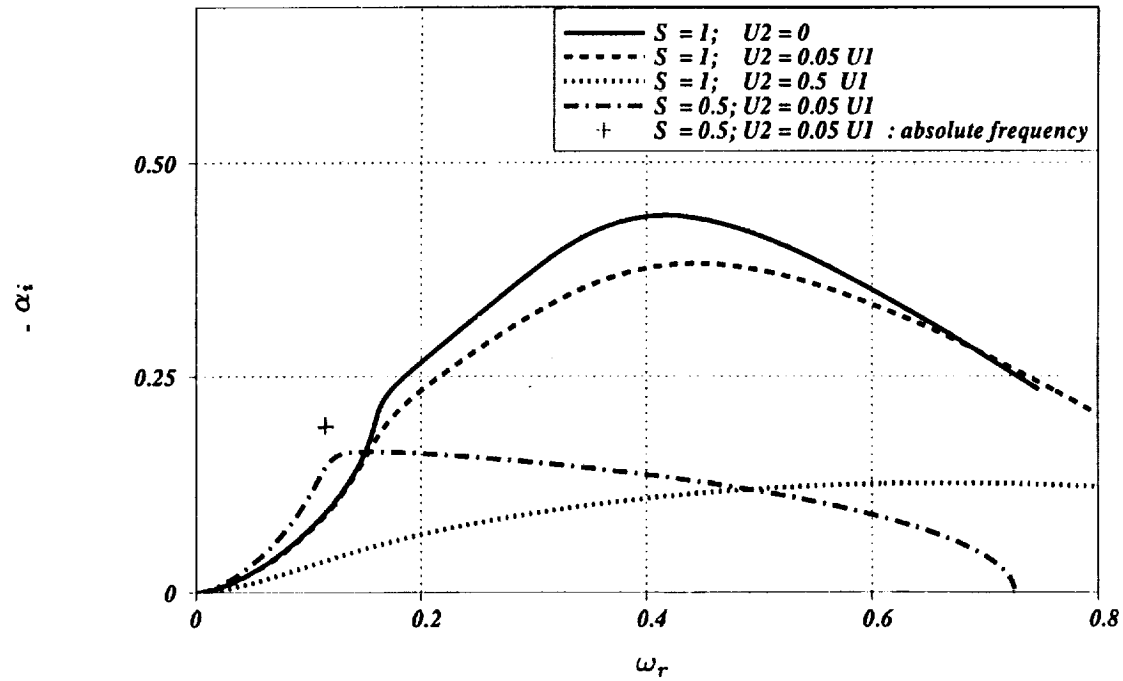

FIGURE 6. Spatial amplification $-\alpha_i$ *versus* real frequency (ω_r) for various co-flows (U_2/U_1) and temperature ratios (S).

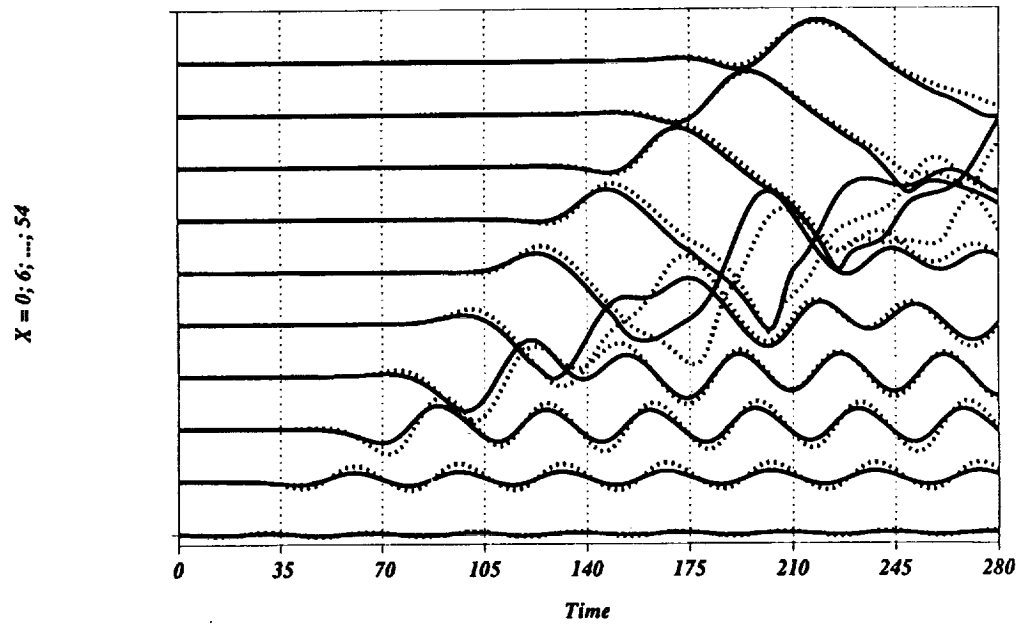

(a)

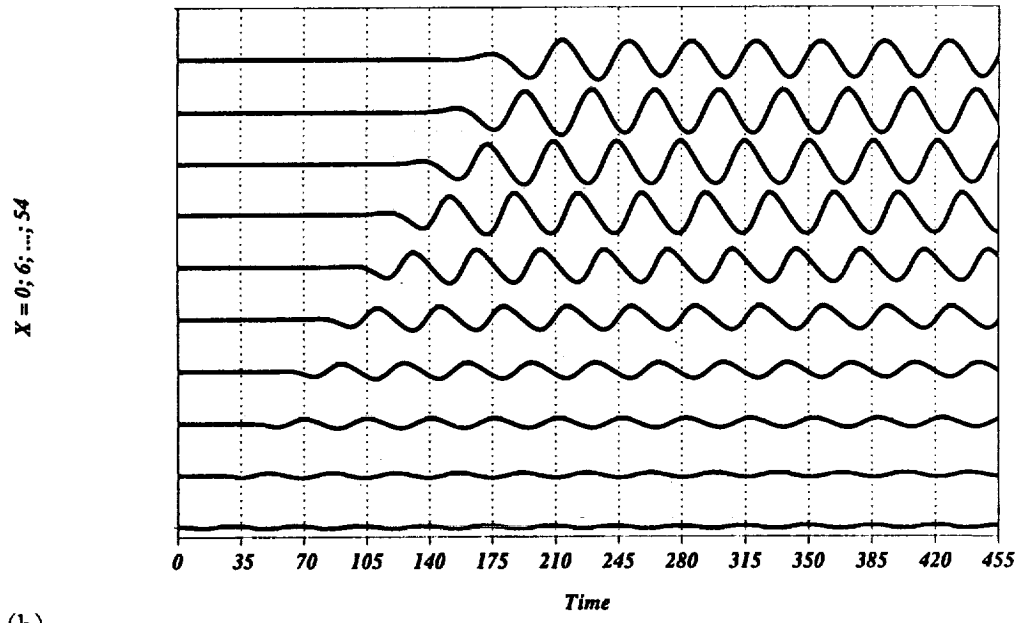

(b)

FIGURE 7. Cold jet ($L_x = 60$): V-velocity history in the shear layer at different x-locations.(a): $A_0 = 5\%$ (solid line) and 10% (dashed line), co-flow: $U_2 = 0.05U_1$; (b): $A_0 = 1\%$, co-flow $U_2 = 0.5U_1$.

to specify the incompressible eigenfunctions which are used as forcing functions. These are:

$$u(y,t) = A(t)\{U_c(y)\cos(\omega_r t) + U_s(y)\sin(\omega_r t)\}$$
$$v(y,t) = A(t)\{V_c(y)\cos(\omega_r t) + V_s(y)\sin(\omega_r t)\}$$

where:

$$A(t) = A_0(1 - e^{-(t/\tau)^2})$$
$$\tau = 10$$

and ω_r is the forcing frequency: $2\pi/\omega_r \approx 35$

The functions U_c, U_s, V_c, V_s which are given by the LIISA are normalized in order to obtain: $A_0 = u_{rms}/U_1$, and u_{rms} is evaluated by averaging over both the cross stream direction and time. These forcing functions are added to the steady inflow profiles. The results of the LIISA and the forcing provide useful information about the simulations which were described in §1.2:

1. The frequency which is observed in the DNS is slightly more than half the most amplified frequency, which means that it lies in the amplified part of the eigenvalue spectrum of the cold jet (see Figure 6). This result supports the idea that the simulated flows amplify physically the numerical noise generated at inflow in a similar way than jets amplify ambient noise in experimental facilities.
2. Forcing the jet at the most unstable frequency does not have any significant effect on the jet if the co-flow is small since the frequency which has been observed without forcing seems to reappear in the downstream half of the box. Furthermore, this tendency remains even at high forcing levels ($A_0 = 5\%$ and 10%) (see Figure 7(a)). Moreover, the level of the perturbations is only controlled in the vicinity of the inflow. If the co-flow is significant ($U_2 = 0.5U_1$), the frequency can be controlled in the whole domain (see Figure 7(b)) even with small forcing levels ($A_0 = 1\%$). This improvement is due to the fact that the stability increases along with the co-flow: thus the flow is not so sensitive to numerical disturbances. Nevertheless, these results prove that the feedback mechanism generates such strong perturbations that there is little hope of controlling them by forcing the inflow in the absolutely and almost absolutely unstable jets. Non-linear saturation occurs less than two diameters downstream.

2.3 Initial conditions

Another natural approach to control the transient is to reduce it by improving the initial conditions (the default initial conditions are obtained by translating the inflow profile through the computational domain). This seems to be a promising idea since we have no possibility of determining the jet entrainment velocity ($V_\infty = V(y_\infty)$) without knowing *a priori* the streamwise evolution of the axial velocity $U_1(x)$ (so far, the initial flows fields have no streamwise evolution). Thus a better estimate of the entrainment velocity than $V_\infty = 0$ could indeed be obtained from an initial flow field which would estimate the evolution of $U_1(x)$. We have examined several ways to achieve this goal.

2.3.1 Analytical or self-similar steady state solution

In the case of mixing layers, transients can be significantly reduced by computing numerically the self-similar steady state which is the solution of the Blasius boundary-layer equation. This has been done successfully for compressible unity-Prandtl number viscous flows by Sandham & Reynolds (1989) and Colonius (1992). For incompressible 2D-jets, a well-known analytic solution has been found by Schlichting (1933), but its validity is restricted to the region where the jet is fully developed. This solution can easily be generalized to compressible jets by using the Howarth (or Illingworth-Stewartson) transform of the cross stream variable:

$$Y_H = \int_0^T \frac{dy}{T}$$

in a similar manner as Sandham & Reynolds (1989) proceeded for 2D compressible mixing layers. Unfortunately, this solution can not be extended to the regions with strong shear (top-hat U-velocity profiles) because the dynamics are governed by two independent spatial scales, the jet diameter and the shear layer thickness. The resulting profile can't be self-similar unless the two spatial scales are identical (this is precisely the case of a fully developed jet which has a Gaussian U-velocity profile) or one of them is disappearing (this is the case of a no co-flowed mixing layer). For similar reasons, the analytic solution can not be extended to co-flowed jets for which U_1 and U_2 are two conflicting velocity scales unless they reduce to a single one. This happens for very small co-flows where the flow differs only slightly from the non-co-flowed case and also for $U_2 \approx U_1$ where the solution should be wake-like. This is in contradiction with Abramovich (1963), who found self-similarity in experimental results.

At any rate, there is neither an analytical nor a self-similar solution for the jet flows which meet the requirements of both the instability issue (top-hat profiles and small co-flows) and the DNS codes ($U_2 > 0$).

2.3.2 Numerical steady-state solution

Since analytical and semi-analytical tools fail to provide the desired steady-state solution, we drew our attention towards purely numerical solutions obtained from a less accurate but more robust code than the ones used so far for DNS. The feasibility of this approach for generation of initial conditions was tested by computing the steady state of strongly co-flowed jets with the Colonius code and zeroth order Giles boundary conditions. Once the steady state was reached, we switched to the more accurate first order boundary conditions. Figure 8 shows that even with a co-flow $U_2 = 0.5\ U_1$, the simple switch to first order boundary conditions generates a new transient which is as intense as the first one. By comparing this figure to Figure 2(a) of our previous report (Jacob (1991)), it turns out that this new transient is as strong as if the first order boundary conditions had been applied directly to the default initial condition.

Since the two codes differ only by their boundary conditions, the steady states reached with each of them are almost identical inside the computational domain.

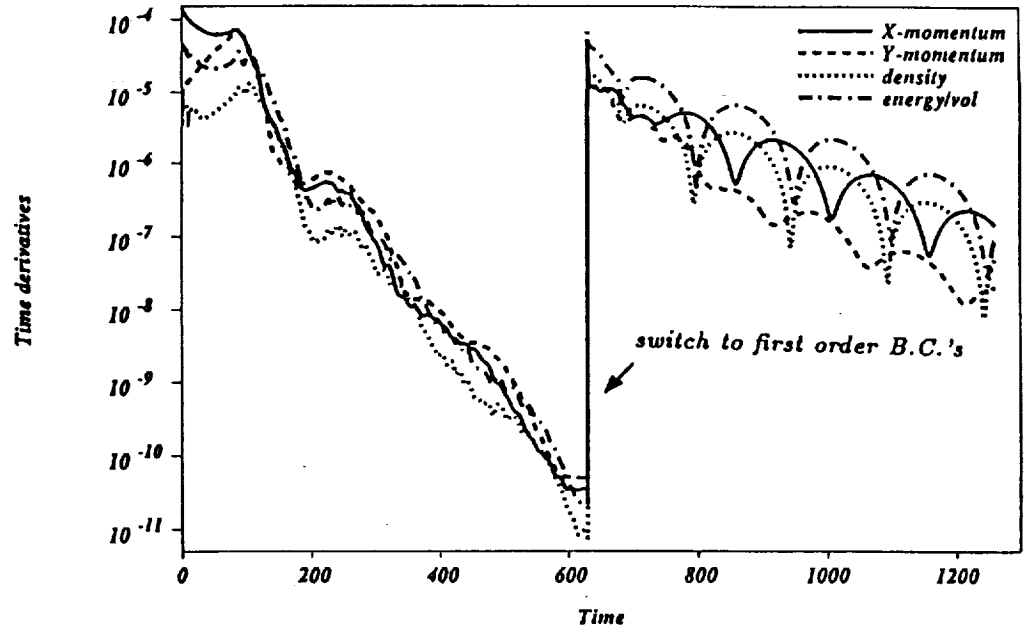

FIGURE 8. Cold jet: History of space averaged time derivatives with switch from zeroth order to first order BC's.

This means that the initial condition is unimportant inside the domain (with respect to the transient) and that the only really important feature is the initial field at the boundaries. This conclusion is consistent with the evolution plots of the field variables (*e.g.* see Figure 3 or 7) because these figures show that the transient originates from the inflow boundary. The switch of boundary conditions has been tested for various co-flows and temperature ratios and always leads to the same conclusions.

2.4 Towards DNS of a two dimensional jet

From the last section, it can be seen that a necessary condition to reduce the transient is to find a better formulation for the inflow boundary condition.

2.4.1 Improved one dimensional inflow boundary conditions

We started with the initial inflow boundary condition from the Poinsot-Lele code. It consists of enforcing the profiles of $U(y)$, $V(y)$ and $T(y)$ only in order to determine the transverse gradients and computing the density from the mass conservation equation *via* the interior variables. The remaining terms (normal gradients) are obtained by the one dimensional boundary conditions on the characteristic variables. They are equivalent to setting:

$$\partial \tilde{U}/\partial t = 0$$

$$\partial \tilde{V}/\partial t = 0$$

$$\partial \tilde{T}/\partial t = 0$$

where : $\tilde{U}$, $\tilde{V}$, and $\tilde{T}$ are one-dimensional variables which are locally tangent to the inflow field. With this formulation, the fields at the boundary differ from the Navier-Stokes solution to which the interior fields tend. Thus strong gradients are generated at the inflow.

In order to smooth the transient, we sought a softer formulation in the spirit of that developed for the outflow in earlier studies (Poinsot & Lele (1992)). Instead of imposing the field variables and setting the time derivatives of their one-dimensional approximation to zero, these quantities are determined by a system of first order differential equations:

$$\partial\tilde{U}/\partial t = \alpha(\tilde{U} - U_\infty)$$

$$\partial\tilde{V}/\partial t = \alpha(\tilde{V} - V_\infty)$$

$$\partial\tilde{T}/\partial t = \alpha(\tilde{T} - T_\infty)$$

This is equivalent to enforcing the profiles of U,V,T upstream of the inflow at a typical distance $L(y) \sim U(y)/\alpha$ and letting them evolve exponentially to the interior fields. Thus the fields at the inflow boundary are less constrained and allow for more continuity in the inflow. A typical magnitude of α is $1/\alpha \sim 10$ time steps. The implementation of these boundary conditions gave promising results (particularly for strongly co-flowed cases, the noise was reduced in the converged state) but would not remove the switch-on transient.

2.4.2 Variable co-flow

Since with these improved boundary conditions the code gives very "clean" solutions for strong co-flows but does not converge to a steady state if the co-flow is small (giving the same type of results as those shown in Figure 1), it seems straightforward to start from a steady strongly co-flowed jet and to gradually reduce the co-flow down to a small value. Thus, the transient leaves the domain when the co-flow is still strong, and the small co-flow is reached with a quiet flow. Such a strategy is possible with our new boundary conditions since they allow for a time-fluctuating inlet profile. First tests indicate that steady states are likely to be reached if the time variation of the co-flow $U_2(t)$ is slow enough (ten to fifteen flow-trough times are necessary) to reduce the co-flow by a factor 2 and if $U_2(t)$ is smooth enough. Even though slight fluctuations remain in the flow, they now appear as perturbations of the mean flow whereas they dominated the flow in earlier simulations. Although they show the flow at different times Figure 9 and Figure 1 may be compared because the magnitude of the perturbations shown on Figure 1 does not change significantly over time as discussed in section 1.2. These tests have to be continued with smaller co-flows in order to determine whether this approach is suitable for the study of jets near the absolute instability limit.

2.4.3 Sponge outflow

In addition to the previously described efforts, we also tried a new version of the Colonius code: the outflow has been considerably improved by inserting between the physical domain and the outflow an exit zone or "sponge" in which disturbances

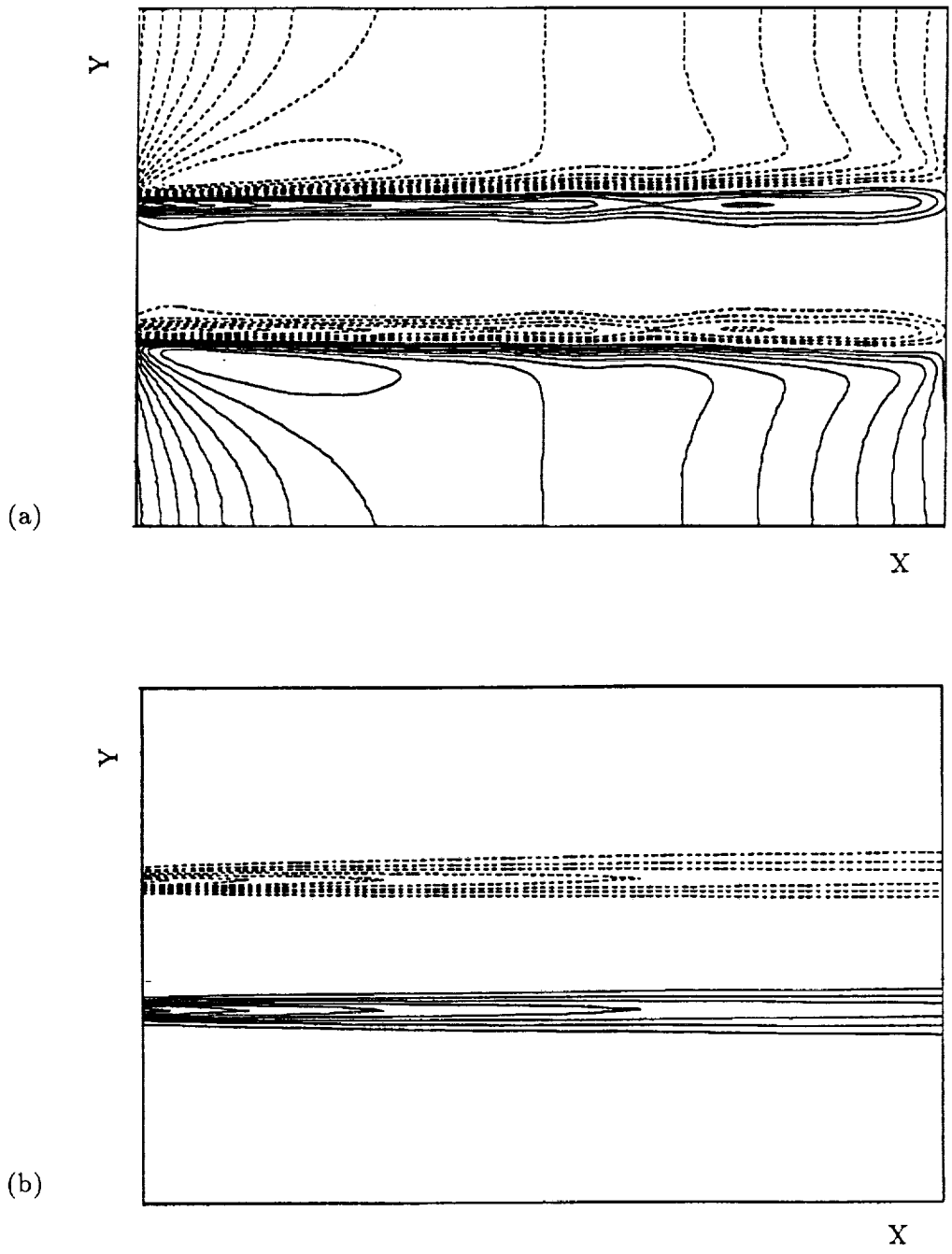

FIGURE 9. Laminar state with reduced co-flow : $U_2 = 0.25U_1$. Contour plots at time= 3000. (a): V-velocity : 10 contour levels : min= −0.00153 , max= 0.00153; (b) : vorticity : 10 contour levels : min= −0.242 , max= 0.0242. Dashed lines are used for negative values in both plots.

are attenuated by grid stretching and filtering (Colonius *et al* (1992)) (as we pointed out in our last year's report the initial two-dimensional first-order Giles boundary conditions were not suited for DNS of slightly co-flowed jets). We tested the case of a cold jet with a co-flow: $U_2 = 0.05U_1$. Even though we extended the domain laterally to a total width of fourteen diameters, the code still blows up as the transient leaves the physical domain since the V-velocity changes its sign on the lateral boundaries when the transient grows. This change from inflow to outflow is not tolerated by the lateral boundary conditions although the amplitude of the disturbance at the lateral boundaries remains small ($< 1\%$ of U_1). In this computation, we started directly with the small co-flow and the default initial conditions for which no entrainment velocity is computed at the lateral boundaries. These remarks already suggest some possible improvements of this simulation.

3. Conclusions

At the present state of this work, there seem to be several ways to obtain a steady state with small co-flows. The first one is to further reduce the co-flow in the Poinsot-Lele code with improved boundary conditions. This might eventually lead to the desired steady state and allow us to examine the issue of absolute instability. However, accurate acoustic fields will not be obtained with that formulation of the boundary conditions. The second choice is to combine some advantages of the two codes: for instance, one could apply the method of co-flow variation to the Colonius code in order to reduce the transient and its effects on the lateral boundaries. One could also reset the reference field for the linearization of the boundary equations once the strongly-coflowed jet has reached its steady state; thus the reference normal V-velocity at the lateral boundaries would be non zero and make these boundary conditions more stable (an increase of the domain width seems not to be a promising approach since this lateral dimension was already considerabely increased in the simulation described in section 2.4.3). The combination of these techniques in the Colonius code seems to be the most promising approach for both an aerodynamical and an aeroacoustical investigation of heated jets (this code already provides good hydrodynamical and aeroacoustical results for spatial mixing layers).

Acknowledgement

I wish to thank Profs. S. K. Lele and P. Moin for their comments and suggestions throughout this work. I am also indebted to Dr. A. Trouvé for the time he spent on this study providing interesting ideas and the LIISA codes which helped me in the ongoing research. Finally I would like to thank Mr. T. Colonius for helping me to test his new code on the jet flow.

REFERENCES

ABRAMOVICH, G. N. 1963 The theory of turbulent jets. *MIT Press Cambridge Massachusetts.*

BERS, A. 1983 Space-time evolution of plasma instabilities - absolute and convective. *In Handbook of Plasma Physics, ed. M. N. Rosenbluth, R. Z. Sagdeev, Amsterdam: North Holland.* **1,** 451-517.

COLONIUS, T., LELE, S. K. & MOIN, P. 1991 Scattering of sound waves by a compressible vortex. *AIAA Paper 91-0494.*

COLONIUS, T., LELE, S. K. & MOIN, P. 1992 Boundary conditions for direct computation of aerodynamic sound. Presented at *DGLR/AIAA 14th aeroacoustic conference, may 11-14, 1992, Aachen, Germany*; also to appear in *AIAA Journal 1993.*

GILES, M. B. 1990 Non reflecting boundary conditions for Euler equation calculations. *AIAA J.* **12,** 2050-2058.

JACOB, M. C. 1991 Direct numerical simulation of instability and noise generation of hot jets *Ann. Res. Briefs,* Center for Turbulence Research, Stanford Univ/NASA Ames.

HUERRE, P., & MONKEWITZ, P. A. 1990 Local and global instabilities in spatially developing flows. *Ann. Rev. Fluid Mech.* **22,** 473-537.

LELE, S. K. 1992 Compact finite difference schemes with spectral-like resolution. *J. Comp. Phys.* **103,** 16-42.

MONKEWITZ, P. A. & SOHN, K. D. 1986 Absolute instability in hot jets and their control . *AIAA Paper 86-1882.*

POINSOT, T. J. & LELE, S. K. 1992 Boundary conditions for direct simulations of compressible viscous reacting flows. *J. Comp. Phys.* **101,** 104.

SANDHAM N. D. & REYNOLDS, W. C. 1989 A numerical investigation of the compressible mixing layer. *Report TF-45,* Thermosciences Division, Department of Mechanical Engineering, Stanford University.

SCHLICHTING,H. 1933 Laminar spread of a jet. *Z. Angew. Math. Mech.* **13,** 260-263.

THOMPSON, K. W. 1989 Time dependant boundary conditions for hyperbolic systems. *J. Comp. Phys.* **68,** 1-24.

TROUVÉ, A. 1988 Instabilités hydrodynamiques et instabilités de combustion de flammes turbulentes, *Thèse de Docteur-ingénieur, Ecole Centrale de Paris.*

YU, M. H. & MONKEWITZ, P. A. 1989 Local and global resonances in heated 2-D jets. *Report for AFOSR grant No. 87-0329.*